



## ABSTRACT

9 Environmental variables are routinely used to forecast when and where an outbreak of tornadoes  
10 is likely to occur but more work is needed to understand how characteristics of severe weather  
11 outbreaks vary with environmental variables. Here the authors propose a method to quantify  
12 ‘outbreak’-level tornado and casualty counts from environmental conditions. They do this by  
13 fitting negative binomial regression models to cluster-level tornado data that estimate tornado  
14 counts and associated casualties on days with at least ten tornadoes. Results show that a 1000 J/kg  
15 increase in CAPE corresponds to a 5% increase in tornado counts and a 28% increase in casualties  
16 holding the other variables constant. Results also show that a 10 m/s increase in deep-layer bulk  
17 shear corresponds to a 13% increase in tornado counts and a 98% increase in casualties holding  
18 the other variables constant. The casualty-count model quantifies the decline in the number of  
19 casualties per year and indicates that tornado outbreaks have a significantly larger impact in the  
20 Southeast than elsewhere after controlling for population and outbreak size.

## 21 **1. Introduction**

22 Predicting specific characteristics of severe weather outbreaks is an important but challenging  
23 problem. Guidance from dynamical models helps forecasters outline areas of severe weather  
24 threats days in advance. Guidance from statistical models help forecasters quantify probabilities  
25 for given severe weather events (Hitchens and Brooks 2014; Thompson et al. 2017; Cohen et al.  
26 2018; Elsner and Schroder 2019; Hill et al. 2020). For example, Cohen et al. (2018) develop a  
27 regression model to specify the probability of tornado occurrence given certain environmental and  
28 storm-scale conditions, and Elsner and Schroder (2019) extend this model by making use of the  
29 cumulative logistic link function that predicts probabilities for each damage rating.

30 These studies put statistical guidance for predicting severe weather outbreak characteristics on a  
31 firm mathematical foundation, yet there is room for additional work. For instance, the cumulative  
32 logistic regression provides a distribution for the *percentage* of tornadoes within each Enhanced  
33 Fujita (EF) rating category, but the regression model is silent concerning the expected overall  
34 number of tornadoes. Here we propose a method to model ‘outbreak’-level tornado and casualty  
35 counts from environmental conditions. The model allows us to quantify the interrelationships  
36 between environmental variables and tornado counts. It also helps in extending the available  
37 statistical guidance because output from a model that estimates the number of tornadoes together  
38 with output from the cumulative logistic model provides a prediction for the expected number of  
39 tornadoes by each EF category. Suppose for example that given current environmental conditions  
40 a model predicts the distribution for the total number of tornadoes centered on fifteen while the  
41 cumulative logistic regression model predicts that for each tornado there is a fifty percent chance  
42 of it being EF0, a ten percent chance of it being EF1, a five percent chance of it being EF2, and

43 so on. Then a numerical convolution of these two distributions provides an expected number of  
44 counts by EF rating as well as the associated uncertainties.

45 This paper has two objectives: (1) to demonstrate that environmental conditions prior to the  
46 occurrence of any tornadoes can be modeled to skillfully estimate the number of tornadoes in a  
47 big outbreak (tornado-count model), and (2) to show that these same environmental conditions  
48 can be used to estimate the number of casualties if the number of people in harm's way is known  
49 (casualty-count model). We accomplish these objects by fitting negative binomial regressions to  
50 cluster-level tornado data. The data are environmental variables and tornado characteristics (e.g.,  
51 number of tornadoes, area of cluster, etc) on 'big' convective days (12 UTC to 12 UTC), when the  
52 number of tornadoes is at least ten (see Elsner and Schroder (2019)).

53 The models show that a  $1000 \text{ J kg}^{-1}$  increase in CAPE results in a 4.7% increase in the expected  
54 number of tornadoes and a 28% increase in the expected number of casualties holding the other  
55 variables constant. Further models show that a  $10 \text{ m s}^{-1}$  increase in deep-layer bulk shear results  
56 in a 13% increase in the expected number of tornadoes and a 98% increase in the expected  
57 number of casualties holding the other variables constant. The casualty-count model also shows a  
58 significant decline in the number of casualties at a rate of 3.6% per year and that expected casualties  
59 depend on where the outbreak occurs with more casualties on average over the Southeast all else  
60 being equal. The paper is outlined as follows. The data and methods are discussed in section 2  
61 including the mathematics of a negative binomial regression. Statistics describing the response  
62 and environmental variables are given in section 3. The modeling results are presented in section  
63 4, and a summary with conclusions are given in section 5.

## 64 2. Data and methods

65 We fit regression models to a set of reanalysis data aggregated to the level of tornado clusters.  
66 Here we describe the available data and the procedures we use to aggregate representative values to  
67 the cluster level. For our purposes, a cluster is a space-time group of at least ten tornadoes occurring  
68 between 12 UTC and 12 UTC. Ten is chosen as a compromise between too few clusters leading  
69 to greater uncertainty and too many clusters leading to excessive time required to fit the models  
70 (Elsner and Schroder 2019). The number of tornadoes in each cluster is the response variable in  
71 the tornado-count regression model, and the number of casualties is the response variable in the  
72 casualty-count regression model. Explanatory variables for the models are taken from reanalysis  
73 data representing the environment before the occurrence of the first tornado in the cluster.

### 74 *a. Tornado clusters*

75 First, we extract the date, time, genesis location, and magnitude of all tornado reports between  
76 1994 and 2018 from the Storm Prediction Center [SPC] (<https://www.spc.noaa.gov/gis/svrgis/>). We choose 1994 as the start year because it is the first year of the extensive use of the  
77 WSR-88D Radar. Each row in the data set contains information at the individual tornado level.  
78 In total, there are 30 497 tornado reports during this period. The geographic coordinates for each  
79 genesis location are converted to Lambert conic conformal coordinates, where the projection is  
80 centered on 107° W longitude.  
81

82 Next, we assign to each tornado a cluster identification number based on the space and time  
83 differences between genesis locations. Two tornadoes are assigned the same cluster identification  
84 number if they occur close together in space and time (e.g., 1 km and 1 h). When the difference  
85 between individual tornadoes and existing clusters surpasses 50 000 s ( $\sim 14$  h), the clustering  
86 ends. The space-time differences have units of seconds because we divide the spatial distance

87 by  $15 \text{ m s}^{-1}$  to account for the average speed of tornado-producing storms. This clustering of  
88 tornadoes is identical to that used in Elsner and Schroder (2019) who fit a cumulative logistic  
89 model to the damage scale at the individual tornado level. Additional details on the procedure as  
90 well as a comparison of the identified clusters to well-known tornado outbreaks are available in  
91 Schroder and Elsner (2019).

92 We keep only clusters that have at least ten tornadoes occurring within the same convective day,  
93 which results in 768 clusters containing a total of 17 069 tornadoes. A convective day is defined as a  
94 24-hour period beginning at 1200 UTC (Doswell III et al. 2006). The average number of tornadoes  
95 (for clusters with at least ten tornadoes) is 22 tornadoes and the maximum is 173 tornadoes (April  
96 27, 2011). There are 80 clusters with exactly ten tornadoes. Each cluster varies by area and by  
97 where it occurs (Fig. 1). The cluster area is defined by the minimum convex hull (black polygon)  
98 that includes all the tornado genesis locations. The July 19, 1994 cluster with nine tornadoes over  
99 northern Iowa and one over northeast Wisconsin had an area of  $33\,359 \text{ km}^2$  and lasted about four  
100 hours. The April 27, 2011 cluster had 173 tornadoes spread over more than a dozen states and  
101 had an area of  $1\,064\,337 \text{ km}^2$  with tornadoes occurring throughout the 24-h period (12-UTC to  
102 12-UTC).

103 For each cluster we sum the number of injuries and deaths across all tornadoes to get the cluster-  
104 level number of casualties. Further we estimate the total population within the cluster area and the  
105 geographic center of the cluster. Population is used as an explanatory variable in place of cluster  
106 area when the number of casualties is the dependent variable.

### 107 *b. Environmental variables*

108 Environmental conditions for producing tornadoes are well known and include high values of  
109 convective available potential energy, convective inhibition, and bulk shear (Brooks et al. 1994;

110 Rasmussen and Blanchard 1998; Tippett et al. 2012, 2014; Elsner and Schroder 2019). We  
111 obtain variables associated with these environmental conditions from the National Centers for  
112 Atmospheric Research’s North American Regional Reanalysis (NARR) which is supported by  
113 the National Centers for Environmental Prediction. Each variable has numeric values given on  
114 a 32-km raster grid with the values available in three-hour increments starting at 00 UTC. We  
115 note that in the severe weather literature these environmental variables are called ‘parameters’.  
116 However here, since we employ statistical models, we prefer to call them variables to be consistent  
117 with the statistical literature where the word ‘parameter’ denotes unknown model coefficients and  
118 distributional moments.

119 We select environmental variables at the nearest three-hour time *prior* to the occurrence of the  
120 first tornado in the cluster. For example, if the first tornado in a cluster occurs at 16:30 UTC we  
121 use the environmental variables given at 15 UTC. This selection criteria results in a sample of the  
122 environment that is less contaminated by the deep convection itself but at a cost that underestimates  
123 the severity in cases where rapid increases in conditions favoring tornadoes occur. We note that  
124 roughly 60% of all clusters have the initial tornado occurring between 18 and 00 UTC (Table 1).  
125 We also note that there are more tornadoes on average in clusters where the first tornado occurs  
126 between 15 and 18 UTC.

127 The environmental variables we consider in this study include convective available potential  
128 energy (CAPE) and convective inhibition(CIN) as computed using the near-surface layer (0 to 180  
129 mb above the ground level) as well as deep (1000 to 500 mb) and shallow (1000 to 850 mb) layer  
130 bulk shears (DLBS, SLBS) computed as the square root of the sum of the squared differences  
131 between the  $u$  and  $v$  wind components at the respective levels. We take the highest (lowest for CIN)  
132 value across the grid of values within the area defined by the cluster’s convex hull. This is done  
133 to capture the extremes of the environmental condition. The maximum values within a cluster

134 provide a better representation of the environments since they are not substantially influenced by  
 135 meso-scale phenomena unrelated to tornado genesis.

136 *c. Negative binomial regression*

137 With the cluster as our unit of analysis we fit a series of regression models to the data having the  
 138 form

$$T \sim \text{NegBin}(\hat{\mu}, n)$$

$$\ln(\hat{\mu}) = \beta_0 + \beta_A A + \beta_\phi \phi + \beta_\lambda \lambda + \beta_Y Y + \beta_{CAPE} CAPE + \beta_{CIN} CIN + \beta_{DLBS} DLBS + \beta_{SLBS} SLBS, \quad (1)$$

139 where the number of tornadoes ( $T$ ) (or number of casualties  $C$ ) is the dependent variable that  
 140 is assumed to be adequately described by a negative binomial distribution (NegBin) with a rate  
 141 parameter  $\mu$  and a size parameter  $n$ . The natural logarithm of the rate parameter is linearly related  
 142 to cluster area ( $A$ ), cluster center location [latitude ( $\phi$ ) and longitude ( $\lambda$ )], year ( $Y$ ) and the four  
 143 environmental variables (CAPE, CIN, DLBS, and SLBS). The model is fit using the method of  
 144 maximum likelihoods carried out in the call to the `glm.nb` function from MASS package in R  
 145 (Venables and Ripley 2002). We do the same for the initial casualty-count model, but we replace  
 146 cluster area with population ( $P$ ). We simplify the initial models by single-term deletions as  
 147 described in §4.

148 **3. Descriptive statistics**

149 The number of clusters decreases exponentially with an increasing number of tornadoes (Fig. 2).  
 150 There are 80 clusters with ten tornadoes but only ten clusters with 30 tornadoes. The right tail of  
 151 the count distribution is long with the April 27, 2011 cluster having 173 tornadoes [47 (6%) of  
 152 the clusters have more than 50 tornadoes and are not shown]. However more clusters have 20 or



153 21 tornadoes than expected from this exponential decay. This deviation is unlikely the result of  
154 physical processes and it appears too large to be sampling variability. The distribution of casualties  
155 is also skewed toward many clusters having only a few casualties and a few have many. Thirty-six  
156 percent of all clusters (275) are without a casualty and 56% of the clusters have fewer than four  
157 casualties.

158 There is a distinct seasonality to the chance of at least one tornado cluster (Fig. 3). The empirical  
159 seven-day probability of at least one cluster is between 20 and 30% for much of the year except  
160 between the middle of March and early July. The probabilities approach 80% between mid and  
161 late May. The number of tornadoes per cluster is less variable ranging between about 10 and 35  
162 tornadoes per week with no strong seasonality although clusters during July and August tend to  
163 have somewhat fewer tornadoes. The casualty rate, defined as the number of casualties per 100,000  
164 people within the cluster area, shows a distinct seasonality with rates being highest between late  
165 January through late May.

166 Across the 768 clusters the mean value of regionally highest CAPE is  $2\,225\text{ J kg}^{-1}$  and the mean  
167 value of regionally lowest CIN is  $-114\text{ J kg}^{-1}$  (Table 2). The maximum deep-layer bulk shear  
168 values range from  $5.6$  to  $47.9\text{ m s}^{-1}$ . Cluster areas range from  $361$  to  $1\,064\,337\text{ km}^2$  with an  
169 average of  $167\,990\text{ km}^2$ .

## 170 **4. Results**

### 171 *a. A model for the number of tornadoes*

172 First we fit a negative binomial regression to the cluster-level tornado counts using the explanatory  
173 variables given in Table 2. This is our tornado-count model. We divide the cluster area by 10  
174 million so it has units of  $100\text{ km}^2$ . We divide CAPE by 1000 so it has units of  $1000\text{ J kg}^{-1}$  and

175 we divide CIN by 100 so it has units of  $100 \text{ J kg}^{-1}$ . This simplifies interpretation of the model  
176 coefficients.

177 All terms have signs on the coefficient that make physical sense (Table 3). The number of  
178 tornadoes in a cluster increases with cluster area, CAPE, and bulk shear (deep and shallow layers)  
179 and decreases for increasing values of CIN as expected. The significance of the variable in  
180 statistically explaining tornado counts is assessed by the corresponding  $z$ -value given as the ratio  
181 of the coefficient estimate to its standard error (S.E.). We reject the null hypothesis that a particular  
182 variable has no explanatory power if its corresponding  $p$ -value is less than .01. Here we fail to  
183 reject the null hypothesis for the variables latitude, longitude, and year, which indicates that these  
184 non-physical variables have a relatively small impact on tornado counts relative to the physical  
185 variables given the data and the model. In particular, there is no significant upward or downward  
186 trend over time in the number of tornadoes in these clusters. The only physical variable that is  
187 not statistically significant is CIN. We remove all statistically insignificant variables before fitting  
188 a final model.

189 All variables in the final model are significant although the coefficients have changed a bit  
190 relative to the initial model. The in-sample correlation between the observed counts and predicted  
191 rates is .59 [(0.54, 0.64), 95% uncertainty interval (UI)] (Fig. 4). The model statistically explains  
192 almost 60% of the variation in cluster-level tornado counts but tends to over predict the number of  
193 tornadoes for smaller clusters and slightly under predict the number of tornadoes for larger clusters.  
194 The mean absolute error between the observed counts and expected rates is 8.6 tornadoes or 5.2%  
195 of the range in observed counts and 9.3% of the range in predicted rates. The out-of-sample  
196 errors are quite similar due to the large sample size (768 clusters). A hold-one-out cross validation  
197 exercise (Elsner and Schmertmann 1994) results in an out-of-sample correlation of .58 and a mean  
198 absolute error of 8.6 tornadoes.

199 The  $\beta_0$  value (Table 3) is the regression estimate when all variables in the model are evaluated at  
200 zero. The effect size for a given explanatory variable is given by the magnitude of its coefficient.  
201 The coefficient is expressed as the difference in the logarithm of the expected tornado counts for  
202 a unit increase in the explanatory variable holding the other variables constant. For example, the  
203 scaled units of CAPE are  $1000 \text{ J kg}^{-1}$ . An increase in CAPE of  $1000 \text{ J kg}^{-1}$  results in a  $[(\exp(.0459)$   
204  $- 1) \times 100\% = 4.7\%$  increase in the expected number of tornadoes. Continuing, units of deep-layer  
205 bulk shear are  $10 \text{ m s}^{-1}$  so an increase in shear of  $10 \text{ m s}^{-1}$  results in a 13% increase in the expected  
206 number of tornadoes. A similar increase in shallow-layer bulk shear results in a 11.1% increase in  
207 the number of tornadoes.

208 Changes to the expected number of tornadoes given changes in the environmental variables  
209 have a large impact on the probability distribution of counts conditional on the cluster area. The  
210 negative binomial distribution for the number of tornadoes  $T$  with an expected number of tornadoes  
211  $\bar{T}$  (obtained from the regression model) has a probability density

$$\Pr(T = k) = \frac{\Gamma(r+k)}{k! \Gamma(r)} \left( \frac{r}{r+\bar{T}} \right)^r \left( \frac{\bar{T}}{r+\bar{T}} \right)^k \quad \text{for } k = 10, 11, 12, \dots, \quad (2)$$

212 where  $r = 1/n$  and  $\Gamma(z) = \int_0^\infty x^{z-1} e^{-x} dx$  is the gamma function.

213 For example, on April 12, 2020 the 12 UTC guidance from SPC outlined a polygon that defined  
214 an area with a 10% chance of at least one tornado occurring within 46 km of any location (10%  
215 tornado risk). The area of the polygon was approximately  $400\,000 \text{ km}^2$  (much larger than the  
216 average cluster area) centered on Mississippi. With an area of that size, the model estimates the  
217 probability of at least 30 tornadoes for a range of deep-layer shear values and conditional on the  
218 amount of CAPE while holding shallow-layer shear at an average value (Fig. 5). Given an average  
219 amount of shallow-layer shear, a deep-layer shear of  $10 \text{ m s}^{-1}$  and low CAPE (5th percentile value),  
220 the model predicts a 17% [9, 26%, UI] chance of at least 30 tornadoes (given a cluster with at least

221 ten tornadoes). In contrast, given a deep-layer shear of  $40 \text{ m s}^{-1}$  and high CAPE (95th percentile  
222 value), the model predicts a 65% [(56, 71%), UI] chance of at least 30 tornadoes. There were at  
223 least 100 tornado numbers on that day.

224 The procedure quantifies the relationship between CAPE and shear in terms of a probability  
225 distribution on the number of tornadoes. The regression model predicts the expected count  
226 given values for the explanatory variables. The negative binomial distribution uses the model  
227 predicted count and the size parameter to generate a distribution of probabilities. For example,  
228 the procedure outputs predicted probabilities across a range of CAPE and deep-layer shear values  
229 (holding shallow-layer shear at its mean value) that provides a high resolution picture of the modeled  
230 relationship (Fig. 6). The predicted probabilities of at least 30 tornadoes given an outbreak covering  
231 an area of  $400\,000 \text{ km}^2$  increase from low values of both CAPE and shear to high values of both  
232 CAPE and shear.

### 233 *b. A model for the number of casualties*

234 Next we fit a negative binomial regression to the cluster-level casualty counts (direct injuries and  
235 deaths) using the same explanatory variables (Table 2) with the exceptions that population (scaled  
236 by 100,000 residents) replaces cluster area and  $C$  (casualty count) replaces  $T$  (tornado count) as  
237 the dependent variable. This is our casualty-count model. We find that CIN is the only variable  
238 not significant in the initial model (Table 4). We remove it before fitting a final model.

239 The in-sample correlation between the observed casualty counts and predicted rates is .43 [(0.37,  
240 .48), 95% UI] (Fig. 7). The mean absolute error between the observed counts and expected rates  
241 is 39 casualties or 1.3% of the range in observed counts and 3.4% of the range in predicted rates.  
242 The out-of-sample correlation is .36 and the mean absolute error is 40 casualties. The skill is

243 lower than the skill of the tornado-count model as there is additional uncertainty associated with  
244 the number of casualties given a tornado.

245 As expected, based on the model for the number of tornadoes, the number of casualties resulting  
246 from a cluster of tornadoes increases with CAPE and with the two bulk shear variables (Table 4).  
247 Holding all other variables constant, an increase in CAPE of  $1000 \text{ J kg}^{-1}$  results in a 28% increase  
248 in the expected number of casualties. An increase in deep-layer bulk shear of  $10 \text{ m s}^{-1}$  results in  
249 a 98% increase in the expected number of casualties and a similar increase in shallow-layer bulk  
250 shear results in a 76% increase in the expected number of casualties. There is also a significant  
251 downward trend (negative value for the  $\beta_Y$  coefficient) in the number of casualties at a rate of 3.6%  
252 per year. This is very likely the result of improvements made by the National Weather Service  
253 in warning coordination and dissemination leading to better awareness especially for these large  
254 outbreak events.

255 Also as expected the number of people in harm's way is a significant predictor for the cluster-level  
256 casualty count. The relationship between population and number of casualties is quantified at the  
257 tornado-level in Elsner et al. (2018) and Fricker et al. (2017) so we expect it to hold at the cluster  
258 level. But here for the first time, we are able to compare the influence of shear and CAPE on the  
259 probability of casualties as modulated by population (Fig. 8). Model results are shown for three  
260 levels of population. The probability of a large number of casualties increases with increasing  
261 shear and increasing CAPE while keeping the other variables at their mean values and year at 2018.

262  
263 Importantly, we also find that the location of the cluster has a significant influence on the number  
264 of casualties. For every one degree north latitude the casualty rate decreases by 5.5% and for every  
265 one degree east longitude the casualty rate increases by 2.9%. Thus cluster-level casualties are  
266 highest over the Southeast. This effect is independent of the number tornadoes since location was

267 not a significant factor in the tornado-count model. The result is also independent of the number  
268 of people in harm's way since population is included as an exploratory variable in the model.

269 To visualize the difference the combine effects of latitude and longitude on the difference in the  
270 probability of many casualties, we plot modeled casualty probabilities (at least 25) as function of  
271 CAPE and deep-layer shear for two *hypothetical* outbreaks that are the same in every way except  
272 one outbreak is center on Sioux City, Iowa and the other is centered on Birmingham, Alabama  
273 (Fig. 9). The modeled probabilities are lowest (around 5%) for low CAPE and shear values and  
274 highest (above 30%) for high CAPE and shear values. The difference in modeled probabilities  
275 across these two locations peaks at about +12 percentage points for high CAPE and high shear  
276 regimes when the outbreak is centered over Birmingham.

## 277 **5. Summary and conclusions**

278 Forecasting characteristics of severe weather outbreaks is challenging. Forecasters use a combi-  
279 nation of numerical weather prediction and empirical guidance to outline areas of severe convective  
280 weather. Machine learning algorithms are now routinely employed for these tasks particularly when  
281 the focus is on prediction rather than on explanation. Here we demonstrate how to employ a statis-  
282 tical regression model to take advantage of the large sample of independent tornado-day events as  
283 a way to parsimoniously predict and importantly to statistically explain the number of tornadoes  
284 and the number of casualties in an outbreak.

285 We fit negative binomial regressions to observational data aggregated to the level of tornado  
286 clusters where a cluster is a space-time group of at least ten tornadoes occurring between 12  
287 UTC and 12 UTC over the period 1994–2018. The number of tornadoes in each cluster is the  
288 response variable in the tornado-count model and the number of casualties (deaths plus injuries)  
289 is the response variable in the casualty-count model. Environmental explanatory variables for the

290 models are extracted from reanalysis data representing conditions before the occurrence of the  
291 first tornado in the cluster. Additional explanatory variables including cluster area, population,  
292 location, and year.

293 The predicted tornado rates explain 59% of the observed tornado counts in-sample, and the  
294 predicted casualty rates explain 43% of the observed casualty counts in-sample. Because of  
295 the large sample size the out-of-sample skill is lower, but still useful. The models show that a  
296  $1000 \text{ J kg}^{-1}$  increase in CAPE results in a 4.7% increase in the expected number of tornadoes and  
297 a 28% increase in the expected number of casualties holding the other variables constant. The  
298 models further show that a  $10 \text{ m s}^{-1}$  increase in deep-layer bulk shear results in a 13% increase  
299 in the expected number of tornadoes and a 98% increase in the expected number of casualties  
300 holding the other variables constant. The casualty-count model also shows a significant decline  
301 in the number of casualties at a rate of 3.6% per year. And casualty rates depend on where the  
302 outbreak occurs with more deaths and injuries, on average, over the Southeast controlling for the  
303 other variables.

304 Some of the unexplained variability in cluster-level tornado counts (and thus casualty counts)  
305 arises from the uncertainty associated with the preferred storm mode and the evolution of meso-  
306 scale convective systems neither of which are captured by a single maximum value in the variable  
307 space of CAPE and shear. Also outbreaks associated with tropical cyclones likely add a bit of noise  
308 to both models since the number of tornadoes is sensitive to the extent and location of convective  
309 bursts within overall evolution of the land-falling storm. In addition, the casualty-count model  
310 would be improved by including a skillful prediction of the number of tornadoes. Indeed in a  
311 perfect-prognostic setting where we know the number of tornadoes in the outbreak, the out-of-  
312 sample correlation between the observed number of casualties and the modeled estimated rate of  
313 casualties increases to .79.

314 A tornado-count model like the one demonstrated here might assist forecast guidance given a  
315 convective outlook that highlights an area of elevated risk for tornadoes and a dynamical forecast of  
316 CAPE and shear across the elevated-risk area. The statistical model would need to be calibrated for  
317 forecast areas and environmental variables but the exact same model equation used here will provide  
318 a probability distribution on the future number of tornadoes that should retain some level of skill.  
319 Further, a numerical convolution of this probability distribution with a probability distribution for  
320 each EF-rating category (Elsner and Schroder 2019) will give a forecast of the expected number  
321 of counts by category as well as the associated uncertainties. Similarly the casualty-count model  
322 might prove useful for communicating the risk given the population within the elevated risk area.

323 The casualty-count model can also be employed in a research setting to help better understand the  
324 socioeconomic, demographic, and communication factors that make some communities particularly  
325 vulnerable to deaths and injuries (Dixon and Moore 2012; Senkbeil et al. 2013; Klockow et al.  
326 2014; Fricker and Elsner 2019). Work along this line has been done at the individual tornado  
327 level by identifying unusually devastating events (Fricker and Elsner 2019) but scaling this type of  
328 analysis to the cluster-level to identify unusually devastating outbreaks might provide additional  
329 insights.

330 Finally, the model specifications might be improved by adjusting the threshold definition of a  
331 cluster. Increasing the threshold on the tornado-count model from 10 to 14 decreases the sample  
332 size to 505 clusters and reduces the effect sizes on CAPE and shear by around 25%. Decreasing  
333 the threshold from 10 to 6 increases the sample size and thus reduces the standard error assuming  
334 the effect size stays the same. The casualty-count model might also be improved by relaxing the  
335 assumption that the number of people injured or killed are independent. Casualties counts are  
336 typically not independent at the household level where multiple people live under the same roof.



337 In this case a zero-inflated count model might be provide a better fit to the data compared with a  
338 negative binomial distribution count model.

339 The negative binomial regression models in this paper were implemented with the `glm.nb`  
340 function from the MASS R package (Venables and Ripley 2002). Graphics were made with the  
341 `ggplot2` framework (Wickham 2017). The code to run all the experiments is available on GitHub  
342 (<https://github.com/jelsner/cape-shear>).

## References

- Brooks, H. E., C. A. Doswell III, and J. Cooper, 1994: On the environments of tornadic and nontornadic mesocyclones. *Weather and Forecasting*, **9**, 606–618, doi:10.1175/1520-0434.
- Cohen, A. E., J. B. Cohen, R. L. Thompson, and B. T. Smith, 2018: Simulating tornado probability and tornado wind speed based on statistical models. *Weather and Forecasting*, **33** (4), 1099–1108, doi:10.1175/waf-d-17-0170.1, URL <https://doi.org/10.1175/waf-d-17-0170.1>.
- Dixon, R. W., and T. W. Moore, 2012: Tornado vulnerability in Texas. *Weather, Climate, and Society*, **4**, 59–68.
- Doswell III, C. A., R. Edwards, R. L. Thompson, J. A. Hart, and K. C. Crosbie, 2006: A simple and flexible method for ranking severe weather events. *Weather and Forecasting*, **21** (6), 939–951, doi:10.1175/waf959.1, URL <https://doi.org/10.1175/waf959.1>.
- Elsner, J. B., T. Fricker, and W. D. Berry, 2018: A model for U.S. tornado casualties involving interaction between damage path estimates of population density and energy dissipation. *Journal of Applied Meteorology and Climatology*, **57**, 2035–2046.
- Elsner, J. B., and C. P. Schertmann, 1994: Assessing forecast skill through cross validation. *Weather and Forecasting*, **9** (4), 619–624.
- Elsner, J. B., and Z. Schroder, 2019: Tornado damage ratings estimated with cumulative logistic regression. *Journal of Applied Meteorology and Climatology*, **58** (12), 2733–2741, doi:10.1175/jamc-d-19-0178.1, URL <https://doi.org/10.1175/jamc-d-19-0178.1>.
- Fricker, T., and J. B. Elsner, 2019: Unusually devastating tornadoes in the United States: 1995–2016. *Annals of the American Association of Geographers*, **110** (3), 724–738, doi:10.1080/24694452.2019.1638753, URL <https://doi.org/10.1080/24694452.2019.1638753>.

365 Fricker, T., J. B. Elsner, and T. H. Jagger, 2017: Population and energy elasticity of tornado  
366 casualties. *Geophysical Research Letters*, **44**, 3941–3949, doi:10.1002/2017GL073093.

367 Hill, A. J., G. R. Herman, and R. S. Schumacher, 2020: Forecasting severe weather with random  
368 forests. *Monthly Weather Review*, doi:10.1175/mwr-d-19-0344.1, URL [https://doi.org/10.1175/  
369 mwr-d-19-0344.1](https://doi.org/10.1175/mwr-d-19-0344.1).

370 Hitchens, N. M., and H. E. Brooks, 2014: Evaluation of the Storm Prediction Center’s convective  
371 outlooks from day 3 through day 1. *Weather and Forecasting*, **29** (5), 1134–1142, doi:10.1175/  
372 waf-d-13-00132.1, URL <https://doi.org/10.1175/waf-d-13-00132.1>.

373 Klockow, K. E., R. A. Pepler, and R. A. McPherson, 2014: Tornado folk science in Alabama  
374 and Mississippi in the 27 April 2011 tornado outbreak. *GeoJournal*, **79** (6), 791–804, doi:  
375 10.1007/s10708-013-9518-6, URL <https://doi.org/10.1007/s10708-013-9518-6>.

376 Rasmussen, E. N., and D. O. Blanchard, 1998: A baseline climatology of sounding-  
377 derived supercell and tornado forecast parameters. *Weather and Forecasting*, **13** (4), 1148–  
378 1164, doi:10.1175/1520-0434(1998)013<1148:ABCOSD>2.0.CO;2, URL [https://doi.org/10.  
379 1175/1520-0434\(1998\)013<1148:ABCOSD>2.0.CO;2](https://doi.org/10.1175/1520-0434(1998)013<1148:ABCOSD>2.0.CO;2).

380 Schroder, Z., and J. B. Elsner, 2019: Quantifying relationships between environmental factors  
381 and power dissipation on the most prolific days in the largest tornado “outbreaks”. *International  
382 Journal of Climatology*, doi:10.1002/joc.6388, URL <https://doi.org/10.1002/joc.6388>.

383 Senkbeil, J. C., D. A. Scott, P. Guinazu-Walker, and M. S. Rockman, 2013: Ethnic and racial  
384 differences in tornado hazard perception, preparedness, and shelter lead time in Tuscaloosa. *The  
385 Professional Geographer*, **66** (4), 610–620, doi:10.1080/00330124.2013.826562, URL [https:  
386 //doi.org/10.1080/00330124.2013.826562](https://doi.org/10.1080/00330124.2013.826562).

- 387 Thompson, R. L., and Coauthors, 2017: Tornado damage rating probabilities derived from WSR-  
388 88D data. *Weather and Forecasting*, **32** (4), 1509–1528, doi:10.1175/waf-d-17-0004.1, URL  
389 <https://doi.org/10.1175/waf-d-17-0004.1>.
- 390 Tippett, M. K., A. H. Sobel, and S. J. Camargo, 2012: Association of U.S. tornado occurrence  
391 with monthly environmental parameters. *Geophysical Research Letters*, **39**, L02 801.
- 392 Tippett, M. K., A. H. Sobel, S. J. Camargo, and J. T. Allen, 2014: An empirical relation between  
393 U.S. tornado activity and monthly environmental parameters. *Journal of Climate*, **27**, 2983–  
394 2999.
- 395 Venables, W. N., and B. D. Ripley, 2002: *Modern Applied Statistics with S*. 4th ed., Springer, New  
396 York, URL <http://www.stats.ox.ac.uk/pub/MASS4>, iISBN 0-387-95457-0.
- 397 Wickham, H., 2017: *tidyverse: Easily Install and Load 'Tidyverse' Packages*. URL [https://CRAN.](https://CRAN.R-project.org/package=tidyverse)  
398 [R-project.org/package=tidyverse](https://CRAN.R-project.org/package=tidyverse), r package version 1.1.1.

399 **LIST OF TABLES**

400 **Table 1.** Cluster statistics by time of day. Each cluster is categorized by the closest  
401 three-hour time (defined by the NARR data) prior to the first tornado. . . . . 22

402 **Table 2.** Variables used in the regression models. Values include the range and average  
403 across the 768 tornado clusters. . . . . 23

404 **Table 3.** Coefficients in the tornado-count models. The size parameter ( $n$ ) is  $6.27 \pm .393$   
405 (S.E.) for the initial model  $6.25 \pm .392$  (S.E.) for the final model. . . . . 24

406 **Table 4.** Coefficients in the casualty-county models. The size parameter ( $n$ ) is  $.261 \pm .014$   
407 (S.E.) for the initial and final models. . . . . 25

408 TABLE 1. Cluster statistics by time of day. Each cluster is categorized by the closest three-hour time (defined  
409 by the NARR data) prior to the first tornado.

Time of Day (UTC)	Number of Clusters	Number of Tornadoes	Tornadoes Per Cluster
00	33	523	15.8
03	5	67	13.4
06	2	23	11.5
12	145	3598	12.1
15	124	3222	26.0
18	249	5220	21.0
21	210	4416	21.0

410 TABLE 2. Variables used in the regression models. Values include the range and average across the 768 tornado  
 411 clusters.

Variable	Abbreviation	Range	Average
Explanatory Variables			
Convective Available Potential Energy [J kg <sup>-1</sup> ]	CAPE	[0, 6530]	2225
Convective Inhibition [J kg <sup>-1</sup> ]	CIN	[-668, 0]	-114
Deep-Layer Bulk Shear [m s <sup>-1</sup> ]	DLBS	[5.6, 48]	27.5
Shallow-Layer Bulk Shear [m s <sup>-1</sup> ]	SLBS	[1.1, 33.8]	15.0
Latitude [° N]	$\phi$	[27.12, 48.97]	37.20
Longitude [° E]	$\lambda$	[-109.9 -72.88]	-92.16
Cluster Area [km <sup>2</sup> ]	$A$	[361, 1 064 337]	167 990
Population [No. of People]	$P$	[0, 38 226 946]	3 387 259
Year	$Y$	[1994, 2018]	2006
Response Variables			
Number of Tornadoes	$T$	[0, 173]	22.2
Number of Casualties (injuries plus deaths)	$C$	[0, 3 069]	29.9

412 TABLE 3. Coefficients in the tornado-count models. The size parameter ( $n$ ) is  $6.27 \pm .393$  (S.E.) for the initial  
 413 model  $6.25 \pm .392$  (S.E.) for the final model.

Coefficient	Estimate	S.E.	$z$ value	$\Pr(> z )$
Initial Model				
$\beta_0$	4.5489	4.7662	0.9540	0.3399
$\beta_A$	0.0146	0.0011	12.80	< 0.0001
$\beta_\phi$	-0.0051	0.0043	-1.17	0.2427
$\beta_\lambda$	-0.0028	0.0031	-0.917	0.3594
$\beta_Y$	-0.0012	0.0024	-0.515	0.6068
$\beta_{CAPE}$	0.0452	0.0153	2.96	0.0031
$\beta_{CIN}$	-0.0110	0.0189	-0.581	0.5612
$\beta_{DLBS}$	0.1256	0.0292	4.30	< 0.0001
$\beta_{SLBS}$	0.1059	0.0355	2.98	0.0029
Final Model				
$\beta_0$	2.1779	0.0817	26.65	< 0.0001
$\beta_A$	0.0149	0.0011	13.85	< 0.0001
$\beta_{CAPE}$	0.0459	0.0146	3.13	0.0017
$\beta_{DLBS}$	0.1254	0.0288	4.35	< 0.0001
$\beta_{SLBS}$	0.1054	0.0314	3.35	0.0008



414 TABLE 4. Coefficients in the casualty-county models. The size parameter ( $n$ ) is  $.261 \pm .014$  (S.E.) for the  
 415 initial and final models.

Coefficient	Estimate	S.E.	$z$ value	$\Pr(> z )$
Initial Model				
$\beta_0$	76.6908	20.7430	3.70	0.0002
$\beta_P$	0.0122	0.0019	6.51	< 0.0001
$\beta_\phi$	-0.0561	0.0187	-3.00	0.0027
$\beta_\lambda$	0.0284	0.0136	2.09	0.0363
$\beta_Y$	-0.0364	0.0103	-3.52	0.0004
$\beta_{CAPE}$	0.2436	0.0643	3.79	0.0002
$\beta_{CIN}$	0.0052	0.0802	0.07	0.9479
$\beta_{DLBS}$	0.6853	0.1262	5.43	< 0.0001
$\beta_{SLBS}$	0.5650	0.1534	3.68	0.0002
Final Model				
$\beta_0$	76.7677	20.6902	3.71	0.0002
$\beta_P$	0.0122	0.0018	6.67	0.0000
$\beta_\phi$	-0.0563	0.0186	-3.02	0.0025
$\beta_\lambda$	0.0287	0.0130	2.20	0.0277
$\beta_Y$	-0.0364	0.0103	-3.53	0.0004
$\beta_{CAPE}$	0.2440	0.0643	3.79	0.0001
$\beta_{DLBS}$	0.6833	0.1253	5.45	0.0000
$\beta_{SLBS}$	0.5631	0.1504	3.74	0.0002

416 **LIST OF FIGURES**

417 **Fig. 1.** Example tornado clusters. Each point is the tornado genesis location shaded by EF rating.  
 418 The black line is the spatial extent of the tornadoes occurring on that convective day and is  
 419 defined by the minimum convex hull encompassing the set of genesis locations. . . . . 27

420 **Fig. 2.** Histograms of the number of clusters by number of tornadoes (A) and number of clusters by  
 421 number of casualties (B). The histograms are right-truncated at 50 to show detail on the left  
 422 side of the distributions. Only clusters with at least ten tornadoes are considered in this study. . . . . 28

423 **Fig. 3.** Probability of a cluster, average number of tornadoes per cluster, and average number of  
 424 casualties per million people per cluster by week of the year. . . . . 29

425 **Fig. 4.** Observed cluster-level tornado counts versus predicted rates from a negative binomial re-  
 426 gression. . . . . 30

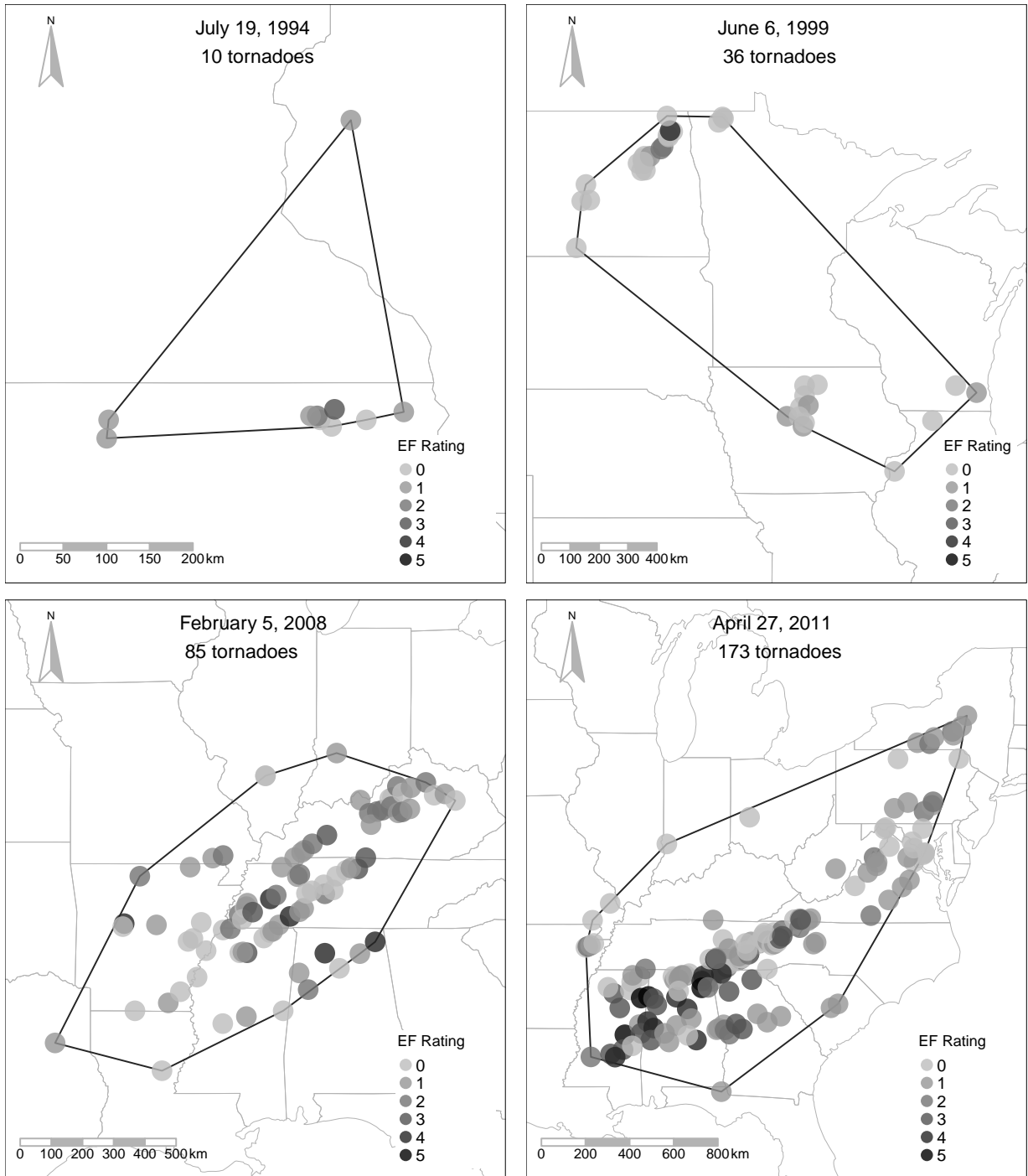
427 **Fig. 5.** Estimated probability of at least 30 tornadoes given an outbreak of at least ten tornadoes  
 428 and the regression model. The predicted count from the model is a parameter in a negative  
 429 binomial distribution with cluster area set at 400 000 km<sup>2</sup> and shallow-level bulk shear is set  
 430 to its mean value. . . . . 31

431 **Fig. 6.** Estimated probability of at least 30 tornadoes given an outbreak of at least ten tornadoes and  
 432 the regression model across a range of CAPE and deep-layer bulk shear values holding the  
 433 shallow-layer bulk shear at a mean value. . . . . 32

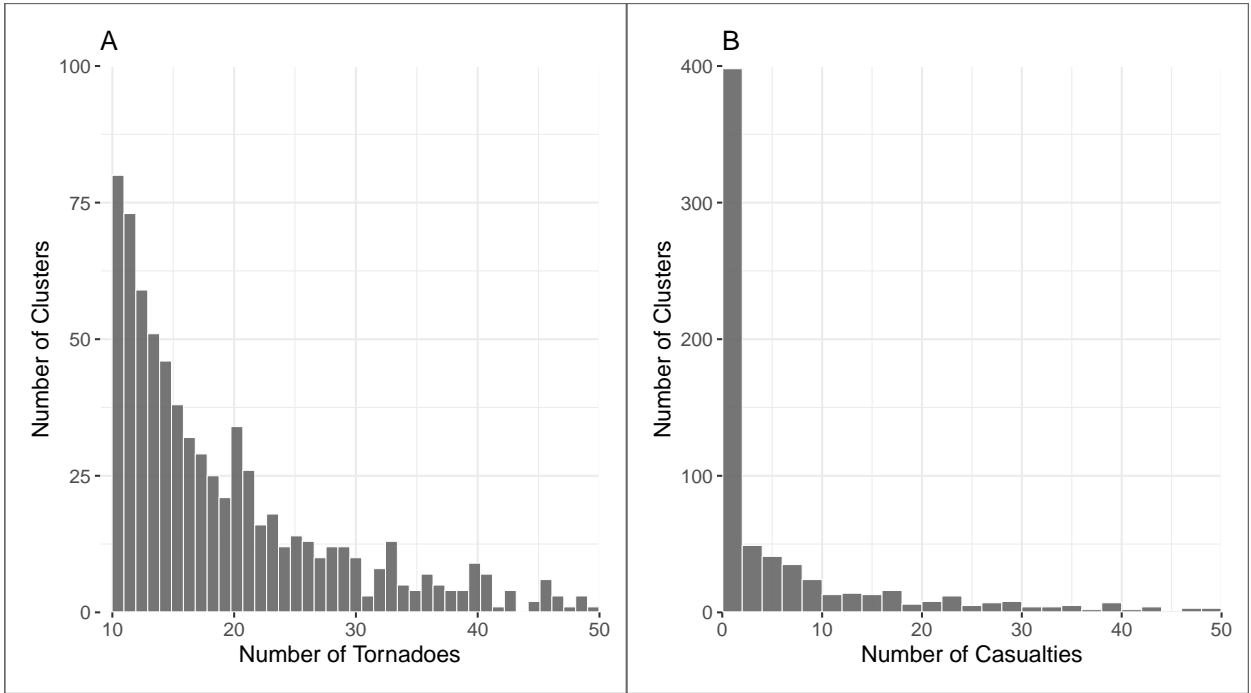
434 **Fig. 7.** Observed cluster-level casualty counts versus predicted rates from a negative binomial re-  
 435 gression. Clusters without casualties are plotted at the far left. . . . . 33

436 **Fig. 8.** Probability of at least 50 tornado casualties as a function of deep-layer bulk shear and CAPE  
 437 and modulated by the number of people in harms way. The other variables are set at their  
 438 mean values and year is set at 2018. . . . . 34

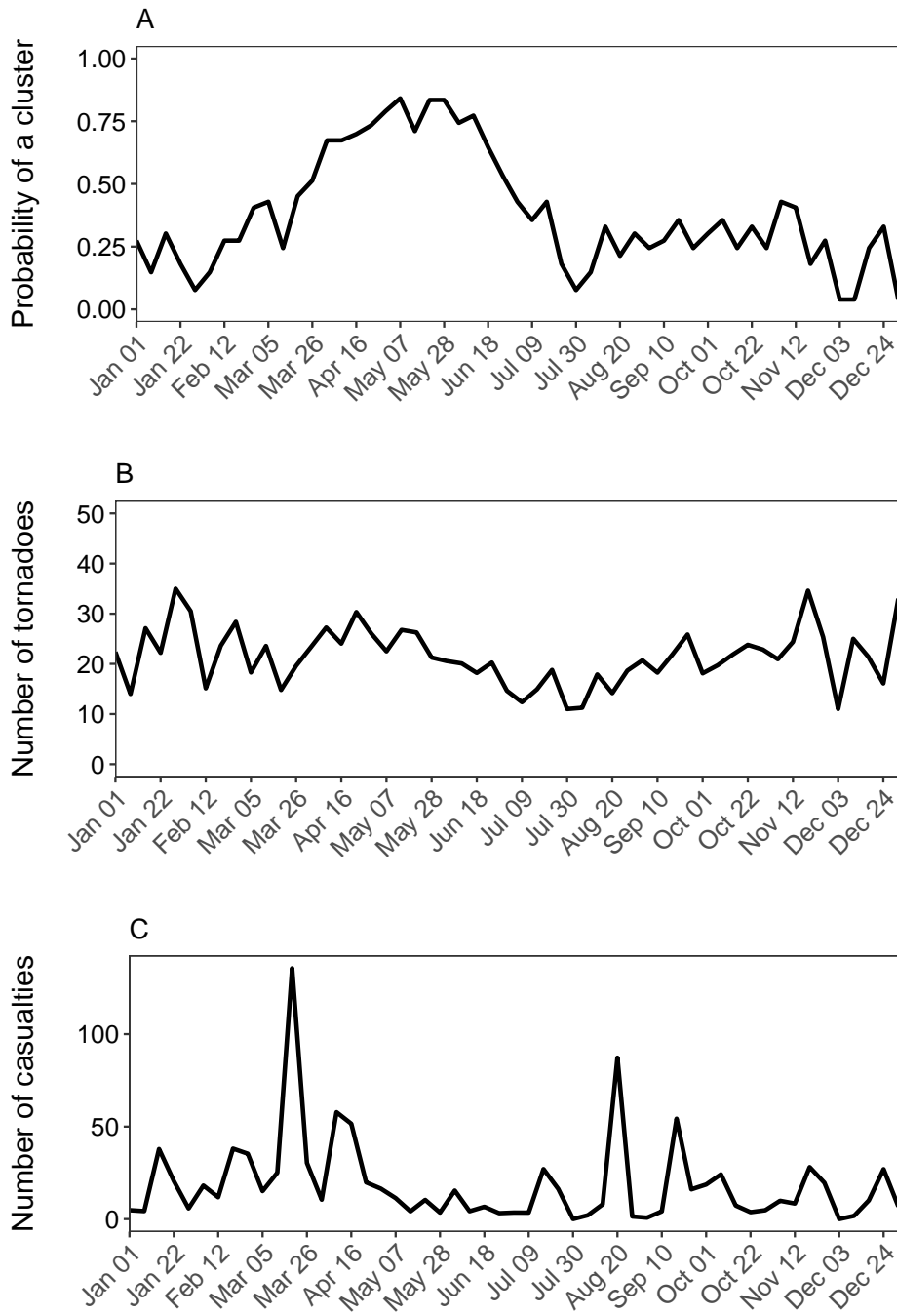
439 **Fig. 9.** Probability of at least 25 tornado casualties as a function of deep-layer bulk shear and CAPE  
 440 and modulated by location for two *hypothetical* outbreaks, one centered over Sioux City,  
 441 Iowa and the other centered over Birmingham, Alabama. The shallow-layer bulk shear is set  
 442 to its mean value, year is set to 2018, and population is set to 4M. . . . . 35



443 FIG. 1. Example tornado clusters. Each point is the tornado genesis location shaded by EF rating. The black  
 444 line is the spatial extent of the tornadoes occurring on that convective day and is defined by the minimum convex  
 445 hull encompassing the set of genesis locations.



446 FIG. 2. Histograms of the number of clusters by number of tornadoes (A) and number of clusters by number of  
 447 casualties (B). The histograms are right-truncated at 50 to show detail on the left side of the distributions. Only  
 448 clusters with at least ten tornadoes are considered in this study.



449 FIG. 3. Probability of a cluster, average number of tornadoes per cluster, and average number of casualties per  
 450 million people per cluster by week of the year.

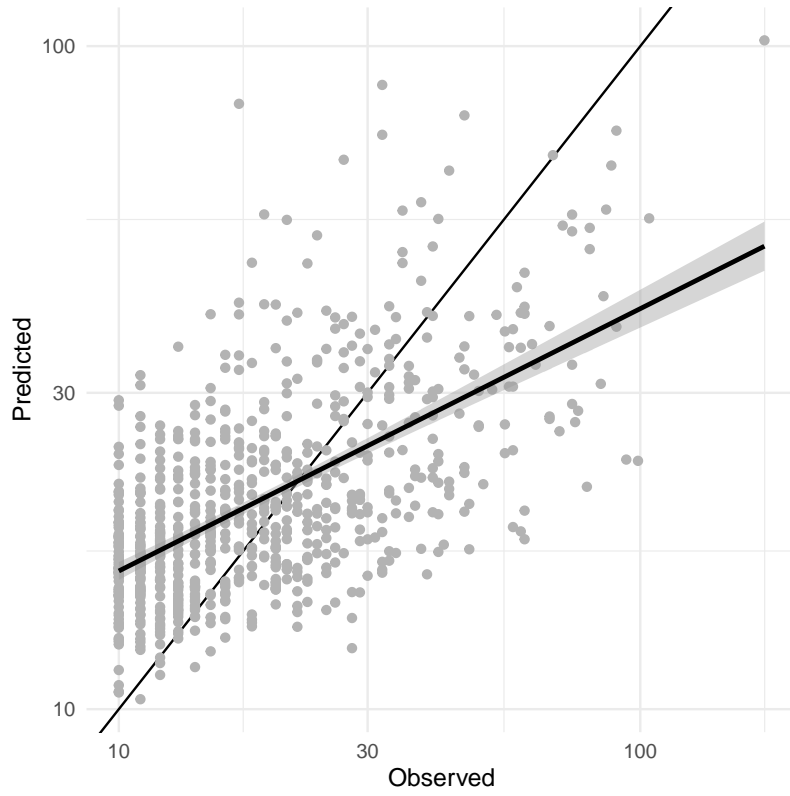
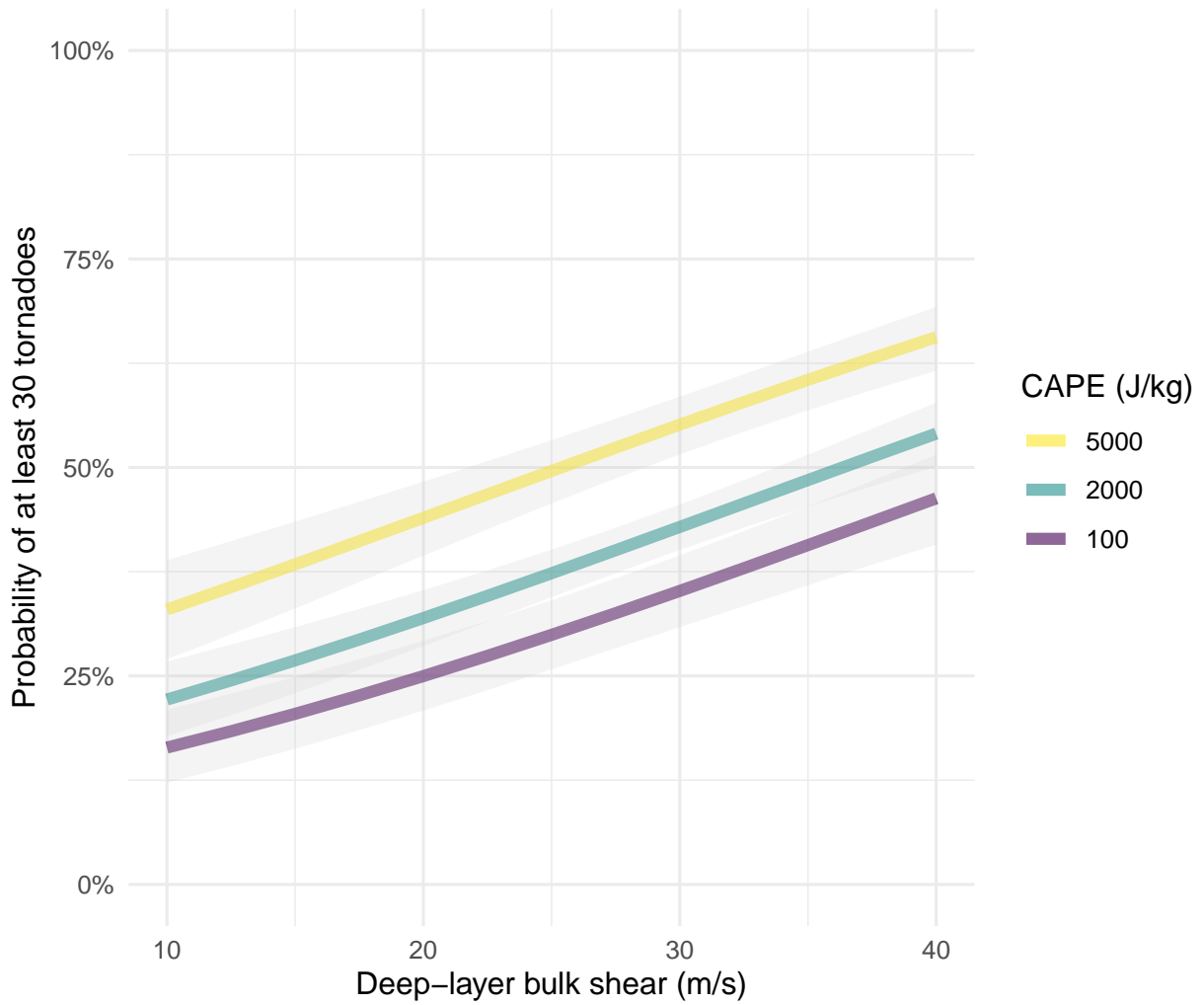
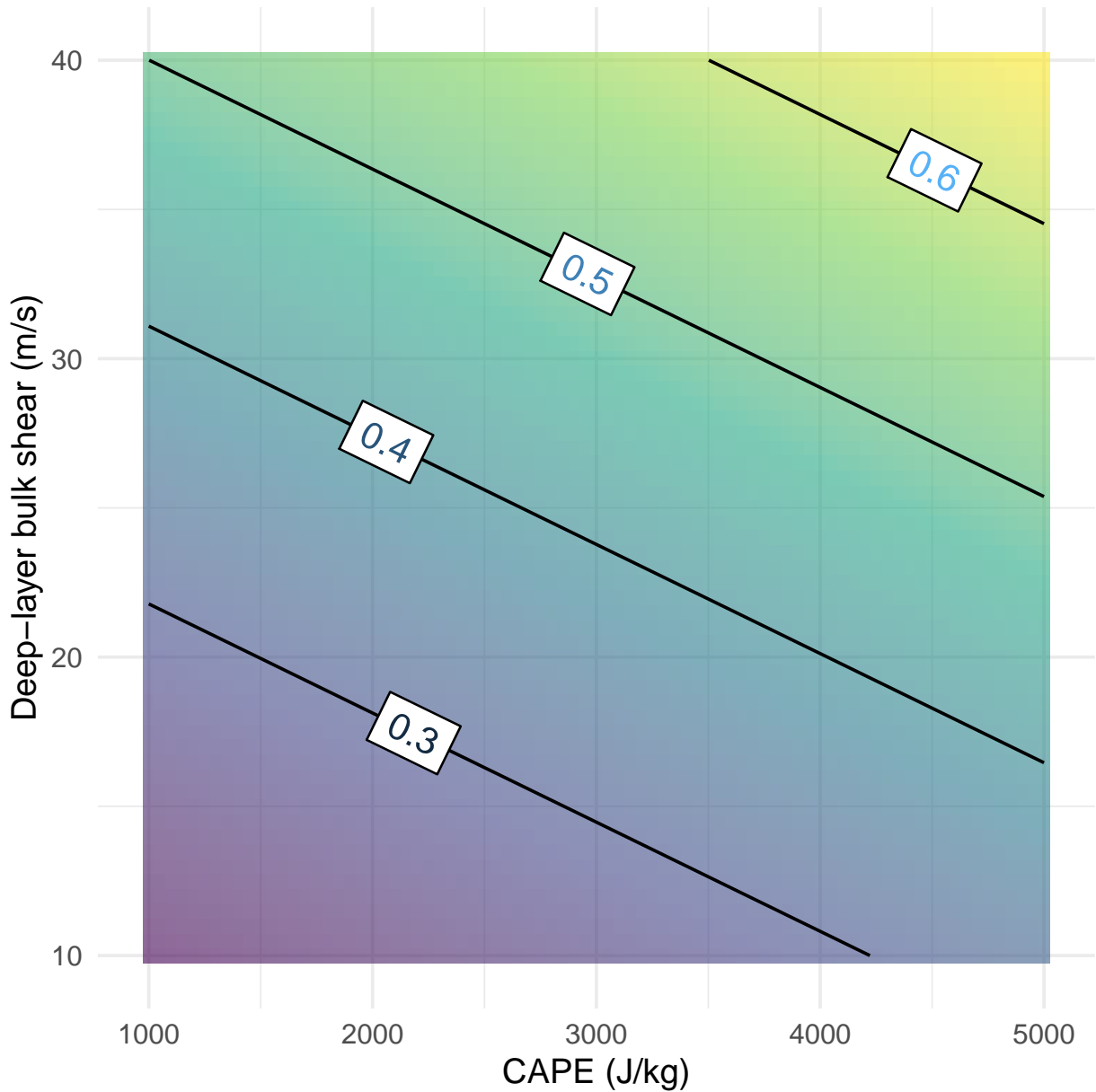


FIG. 4. Observed cluster-level tornado counts versus predicted rates from a negative binomial regression.

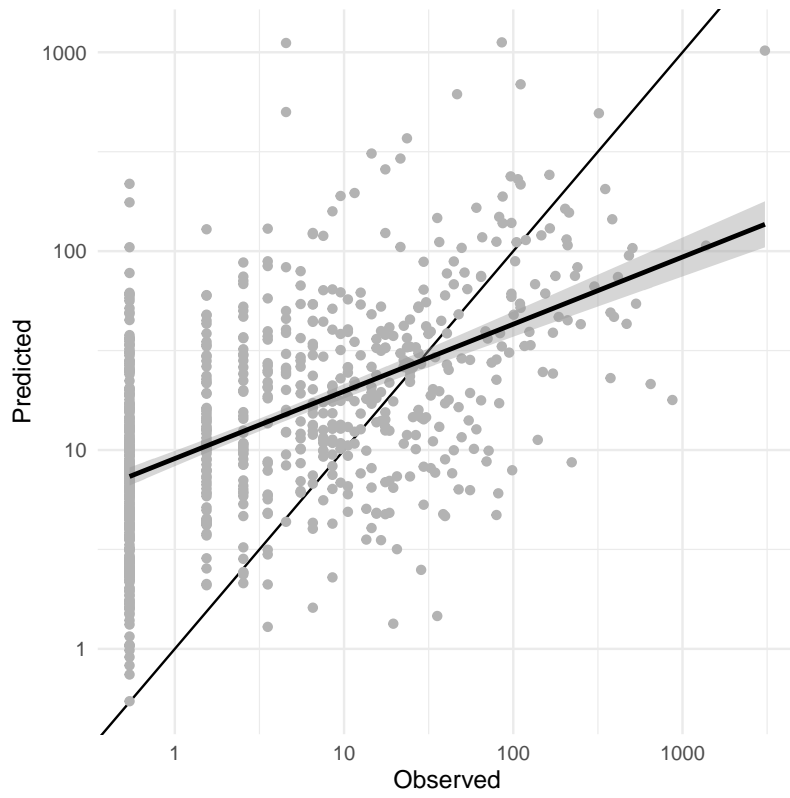


451 FIG. 5. Estimated probability of at least 30 tornadoes given an outbreak of at least ten tornadoes and the  
 452 regression model. The predicted count from the model is a parameter in a negative binomial distribution with  
 453 cluster area set at 400 000 km<sup>2</sup> and shallow-level bulk shear is set to its mean value.

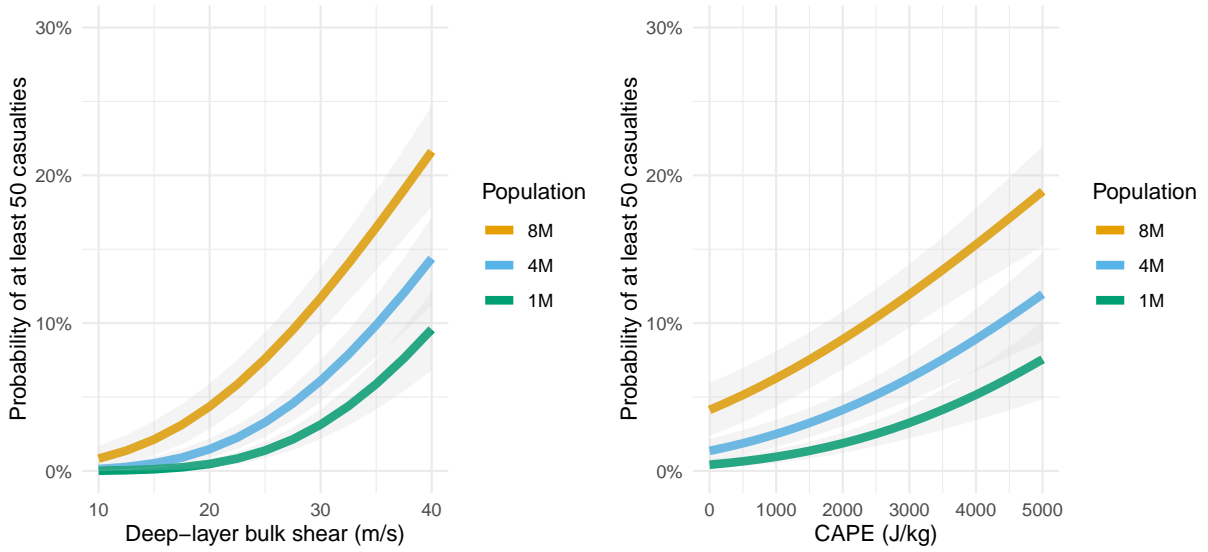


454 FIG. 6. Estimated probability of at least 30 tornadoes given an outbreak of at least ten tornadoes and the  
 455 regression model across a range of CAPE and deep-layer bulk shear values holding the shallow-layer bulk shear  
 456 at a mean value.

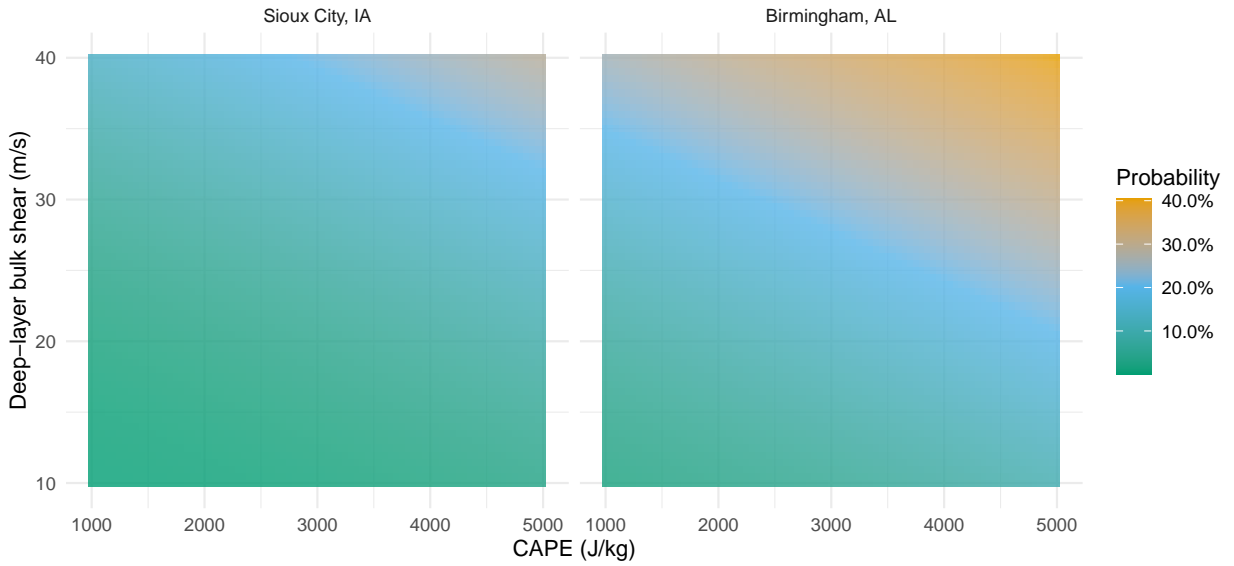




457 FIG. 7. Observed cluster-level casualty counts versus predicted rates from a negative binomial regression.  
458 Clusters without casualties are plotted at the far left.



459 FIG. 8. Probability of at least 50 tornado casualties as a function of deep-layer bulk shear and CAPE and  
 460 modulated by the number of people in harms way. The other variables are set at their mean values and year is set  
 461 at 2018.



462 FIG. 9. Probability of at least 25 tornado casualties as a function of deep-layer bulk shear and  
 463 modulated by location for two *hypothetical* outbreaks, one centered over Sioux City, Iowa and the other centered  
 464 over Birmingham, Alabama. The shallow-layer bulk shear is set to its mean value, year is set to 2018, and  
 465 population is set to 4M.